Biogeosciences, 10, 6591–6600, 2013
www.biogeosciences.net/10/6591/2013/
doi:10.5194/bg-10-6591-2013

Biogeosciences Open Access

Deep CO_2 soil inhalation / exhalation induced by synoptic pressure changes and atmospheric tides in a carbonated semiarid steppe

E. P. Sánchez-Cañete[1,2], A. S. Kowalski[2,3], P. Serrano-Ortiz[1,2], O. Pérez-Priego[2,3], and F. Domingo[1]

[1]Departamento de Desertificación y Geo-ecologia, EEZA-CSIC, Ctra. Sacramento s/n, 04120, La cañada de San Urbano, Almería, Spain
[2]Centro Andaluz de Medio Ambiente (CEAMA), 18006, Granada, Spain
[3]Departamento de Física Aplicada, Universidad de Granada, Av. Fuentenueva s/n, 18071 Granada, Spain

Correspondence to: E. P. Sánchez-Cañete (enripsc@ugr.es)

Received: 17 January 2013 – Published in Biogeosciences Discuss.: 21 March 2013
Revised: 5 September 2013 – Accepted: 6 September 2013 – Published: 18 October 2013

Abstract. Knowledge of all the mechanisms and processes involved in soil CO_2 emissions is essential to close the global carbon cycle. Apart from molecular diffusion, the main physical component of such CO_2 exchange is soil ventilation. Advective CO_2 transport, through soil or snow, has been correlated with the wind speed, friction velocity or pressure (p). Here we examine variations in subterranean CO_2 molar fractions (χ_c) over two years within a vertical profile (1.5 m) in a semiarid ecosystem, as influenced by short-timescale p changes.

Analyses to determine the factors involved in the variations in subterranean χ_c were differentiated between the growing period and the dry period. In both periods it was found that variations in deep χ_c (0.5–1.5 m) were due predominantly to static p variations and not to wind or biological influences. Within a few hours, the deep χ_c can vary by fourfold, showing a pattern with two cycles per day, due to p oscillations caused by atmospheric tides. By contrast, shallow χ_c (0.15 m) generally has one cycle per day as influenced by biological factors like soil water content and temperature in both periods, while the wind was an important factor in shallow $\chi_c$variations only during the dry period. Evidence of emissions was registered in the atmospheric boundary layer by eddy covariance during synoptic pressure changes when subterranean CO_2 was released; days with rising barometric pressure – when air accumulated belowground, including soil-respired CO_2 – showed greater ecosystem uptake than days with falling pressure. Future assessments of the net ecosystem carbon balance should not rely exclusively on Fick's law to calculate soil CO_2 effluxes from profile data.

1 Introduction

The characterization of the different mechanisms and processes involved in soil CO_2 emissions to the atmosphere is important for improving understanding of the global carbon cycle. Respiration is generally the only process considered by the FLUXNET community when modeling or interpreting soil–atmosphere CO_2 exchanges (Falge et al., 2002), presumably transported by molecular diffusion. Recently however, numerous studies of semiarid ecosystems have shown the importance in the net ecosystem carbon balance (NECB; Chapin et al., 2006) of other, abiotic components (Emmerich, 2003; Kowalski et al., 2008; Mielnick et al., 2005; Plestenjak et al., 2012; Rey et al., 2012a; Serrano-Ortiz et al., 2010; Were et al., 2010).

Most researchers interpret soil CO_2 effluxes at the soil surface in terms of concurrent respiration, neglecting subterranean CO_2 storage. Ventilation (gas advection through porous media) can decouple the soil CO_2 source from emissions to the atmosphere with changes in pressure, wind or friction velocity. Scientists have confirmed subterranean advective transport in laboratories (Nachshon et al., 2012; Maier et al., 2012), soils (Clemets and Wilkening, 1974; Maier et al., 2010; Subke et al., 2003; Weisbrod et al., 2009), peatlands (Comas et al., 2005; Comas et al., 2007; Comas et al., 2011), and snow (Bowling and Massman, 2011; Fujiyoshi et al., 2010; Seok et al., 2009; Massman et al., 1997). Some have applied the gradient method – based on Fick's law for molecular diffusion – to model exchange with the atmosphere during calm conditions, but highlight the importance of advective transport in exchanges at other times.

Advective transport of CO_2 through soil or snow has been correlated with changes in subterranean CO_2 molar fractions (χ_c) in conjunction with variations in wind speed, friction velocity or barometric pressure (p). Advection has been detected using isotopic methods (Bowling and Massman, 2011), buried p sensors (Maier et al., 2010; Takle et al., 2004), ^{222}Rn concentrations (Clemets and Wilkening, 1974; Fujiyoshi et al., 2010), ground-penetrating radar (Comas et al., 2005) or variations in CO_2 and other gases (Seok et al., 2009; Hirsch et al., 2004; Reicosky et al., 2008). Even in volcanoes the atmospheric p has a strong influence on both CO_2 degassing (Rogie et al., 2001) and the CO_2 soil efflux (Granieri et al., 2003), as well as on their combination as measured by eddy covariance (Lewicki et al., 2008; Lewicki et al., 2007).

Besides molecular diffusion, the main physical process affecting soil–atmosphere CO_2 exchange is ventilation driven by pressure pumping. Pressure pumping is caused by atmospheric processes including short-period turbulence, longer-period barometric changes and quasi-static pressure fields induced by wind (Massman et al., 1997). Subterranean convection, with CO_2-rich air subsiding due to its enhanced density (Kowalski and Sanchez-Canete, 2010), may also play a role. Most studies attribute gas advection to two atmospheric mechanisms: quasi-static pressure fields and short-period atmospheric turbulence (Huwald et al., 2012), neglecting longer-period barometric changes.

At a nearby experimental site, it was found that wind provoked deep CO_2 emissions to the atmosphere (Sanchez-Canete et al., 2011). Also, at this very experimental site, the wind was found to be the main driver of large CO_2 emissions to the atmosphere (Rey et al., 2012a), suggesting a possible geothermal origin (Rey et al., 2012b). Given these precedents, our objective was to determine the main drivers involved in subterranean CO_2 ventilation and thereby improve knowledge of this little-studied process. Hypothesizing that these CO_2 emissions to the atmosphere could be the result of CO_2 transported from depth towards the surface, we installed a vertical soil profile to monitor subterranean CO_2 variations at depth (0.15, 0.5 and 1.5 m) during two years in this semiarid ecosystem.

2 Material and methods

2.1 Study site

The study was conducted in Balsa Blanca within the Cabo de Gata-Níjar Natural Park of southeast Spain (36° 56′26.0″ N, 2° 0.1′58.8″ W). This is an alpha grass steppe situated on an alluvial fan (glacis) at 200 m a.s.l. The soil is classified as Calcaric Lithic Leptosol (WRB, 2006) saturated in carbonates (0.15 m) over petrocalcic horizons overlying marine carbonate sediments with the presence of fissures and fractures not visible above ground, and volcanic rocks. The texture is sandy loam with sand (61.1 %), silt (22.8 %) and clay (16.1 %) with a bulk density of 1.25 (g cm^{-3}). The climate is dry subtropical semiarid, with a mean annual temperature (T) of 18 °C and precipitation of ca. 200 mm. The ground water level of the main aquifer of Balsa Blanca is situated at a depth of 140 m. The most abundant ground cover is bare soil, gravel and rock (49.1 %), and vegetation is dominated by *Macrochloa tenacissima* (57 % of cover) with other species present, including *Chamaerops humilis*, *Rhamnus lycoides*, and *Pistacia lentiscus*; the vegetation is most active during winter (January–April). More detailed site information is given by Rey et al. (2012a).

2.2 Field measurements

A vertical soil profile was installed in January 2010 to measure CO_2 molar fractions, temperature, and humidity at three depths that we characterized as "shallow" (0.15 m; A horizon), and "deep" (0.5 and 1.5 m; caliche horizon). Here, "deep" is used merely to distinguish between measured horizons, recognizing that all sensors are quite close to the surface. Sensors oriented horizontally in the profile included CO_2 molar fraction (χ_c) probes (GMP-343, Vaisala, Inc., Finland) with soil adapters and hydrophobic filters, thermistors (107 temperature sensor, Campbell Scientific, Logan, UT, USA; hereafter CSI) and water content reflectometers (CS616, CSI) to measure the soil water content (SWC, m^3 m^{-3}). The GMP343 sensors were configured at 25 °C and 1013 hPa and corrected in post-processing for variations in T and pressure. Measurements were made every 30 s and stored as 5 min averages by a data-logger (CR23X, CSI).

Ecosystem-scale CO_2 fluxes were measured by eddy covariance atop a 3.5 m tower. An open-path infrared gas analyzer (Li-Cor 7500, Lincoln, NE, USA) – calibrated monthly – measured barometric pressure (p) and densities of CO_2 and water vapor. A three-axis sonic anemometer (CSAT-3, CSI) measured wind speed and sonic temperature. At 1.5 m above ground level, two quantum sensors (LI-190, Li-Cor) measured incident and reflected photon fluxes. A data-logger (CR3000, CSI) managed the measurements and recorded data at 10 Hz (quantum sensors, storing only half-hour means). Turbulent fluxes were computed every half-hour according to Reynolds rules of averaging, corrected for dry air molar density variations (Webb et al., 1980) and coordinate rotation (Kowalski et al., 1997). The friction velocity (u_*) is determined as the turbulent velocity scale resulting from square root of the kinematic momentum flux (Stull, 1988). Quality control of the eddy flux data was performed according to Serrano-Ortiz et al. (2009).

2.3 Statistical analyses

To study the effect of longer-period barometric changes (atmospheric tides and synoptic events) and the friction velocity versus subterranean CO_2 variations, these variables were

Table 1. Mean ± standard error of soil CO_2 molar fractions (χ_c), soil temperatures (T), soil water contents (SWC), friction velocity (u_*), barometric pressure and air temperature during growing (March / April) and dry (July / August) periods of 2010 and 2011.

	Depth	χ_c	Soil T	SWC	Pressure	Air T	u_*
March–April	0.15 m	514.8 ± 3.3	15.6 ± 0.1	11.1 ± 0.1	987.7 ± 0.1	14.3 ± 0.1	0.4 ± 0.0
	0.5 m	943.3 ± 7.1	15.7 ± 0.0	11.6 ± 0.0			
	1.5 m	813.2 ± 7.4	15.5 ± 0.0	15.3 ± 0.0			
July–August	0.15 m	473 ± 4.0	30.8 ± 0.0	1.4 ± 0.0	986.3 ± 0.1	25 ± 0.1	0.4 ± 0.0
	0.5 m	1114.9 ± 11.2	29.4 ± 0.0	7.2 ± 0.0			
	1.5 m	1142 ± 12.6	26.1 ± 0.0	13.7 ± 0.0			

normalized. This is because different variables are not strictly comparable due to extreme seasonal variations in both means and variances. Additionally, high-pass filtering was applied using two cut-off values to examine both diurnal and synoptic relationships. The normalized data (standardized anomalies; Wilks, 2006) for any meteorological variable are then given by

$$N_i = \left(X - \overline{X_i}\right)/\sigma_i, \quad (1)$$

where N_i is the normalized value, X the measurement, $\overline{X_i}$ the running mean for a window of width i (0.5 or 3 days, diurnal and synoptic timescale, respectively) centered on the time of measurement, and σ_i the standard deviation over the same window. Correlations (R^2) were then examined for both $N_{0.5}$ and N_3 and for two different vegetative periods: the growing period, where the vegetation is most active (March–April), and the dry period, where the vegetation is mostly dormant (July–August). Daytime half-hour data were fitted using an empirical hyperbolic light-response model (Falge et al., 2001) to describe the dependence of CO_2 ecosystem exchange [F_C, µmol m^{-2} s^{-1}] on the incident photon flux [F_P, µmol m^{-2} s^{-1}]:

$$F_C = -\frac{\alpha\beta F_P}{\alpha F_P + \beta} + \gamma, \quad (2)$$

where α (µmol C J^{-1}) is the canopy light utilization efficiency and represents the initial slope of the light-response curve, β (µmol C m^{-2} s^{-1}) is the maximum CO_2 uptake rate of the canopy at light saturation and γ (µmol C m^{-2} s^{-1}) is the ecosystem respiration during the day. All parameters are positive as defined.

3 Results

3.1 Seasonal and interannual patterns

Clear annual patterns are evident in the average daily values of soil temperature (T), water content (SWC), and CO_2 molar fraction (χ_c) at 0.15 m ("shallow") as well as at 0.5 m and 1.5 m depths ("deep"; Fig. 1). Shallow-soil T has its maximum (ca. 34 °C) in summer (June, July and August) and minimum (5 °C) in winter (December, January and February); the SWC shows inverse correlation with T, with basal values near 5 % in summer but often more than 20 % in winter.

Soil CO_2 molar fractions (χ_c) generally increase with depth, with a constant baseline for each horizon over the years, but also with periodic surges to more than double the mean value within a few days. The two deep sensors behave similarly (Fig. 1c), with the blue line (1.5 m depth) overlapping the red line (0.5 m depth) so nearly that the 0.5 m data are practically obscured. They show clear annual patterns with maxima in summer and minima in winter, similar means over the two years ($\chi_c \sim 1032$ ppm at 0.5 m, and 994 ppm at 1.5 m) and rapid variability. By contrast, the shallow sensor (Fig. 1d) has about half the mean ($\chi_c \sim$ 529 ppm CO_2) and notably less variability - in both frequency and magnitude. Also in contrast to the deep case, shallow-soil χ_c is highest in winter and lowest in summer. Differences between the deep and shallow probes are less pronounced in winter. Pressure (p) varies from 967–1007 hPa (Fig. 1e), with increased variability in winter due to the passage of synoptic systems, and suppressed variability in summer under the Mediterranean high. To clarify the relation between χ_c and p, we focus on two different periods of 2011 (Fig. 1. Red rectangles): the growing period from March to May and the dry period from July to September.

3.2 Synoptic patterns

Table 1 shows the mean and standard error of environmental variables associated with varying soil CO_2 molar fractions (χ_c) during both periods. For the growing period (from March to May) deep-soil CO_2 molar fractions (χ_c) are nearly double ($\chi_c \sim$ 943 ppm at 0.5 m, and 813 ppm at 1.5 m) the shallow χ_c ($\sim$ 515 ppm at 0.15 m). At all depths the soil temperature has a similar mean (15.6 °C, 15.7 °C and 15.5 °C at 0.15 m, 0.5 m and 1.5 m, respectively) as can be appreciated in Fig. 1a, and the soil water content increases with depth with values of 11.1 %, 11.6 %, and 15.3 %. During the dry period (from July to September) the deep-soil CO_2 molar fractions (χ_c) are more than double ($\chi_c \sim 1115$ ppm at 0.5 m, and 1142 ppm at 1.5 m) that of the shallow layer ($\sim$ 473 ppm

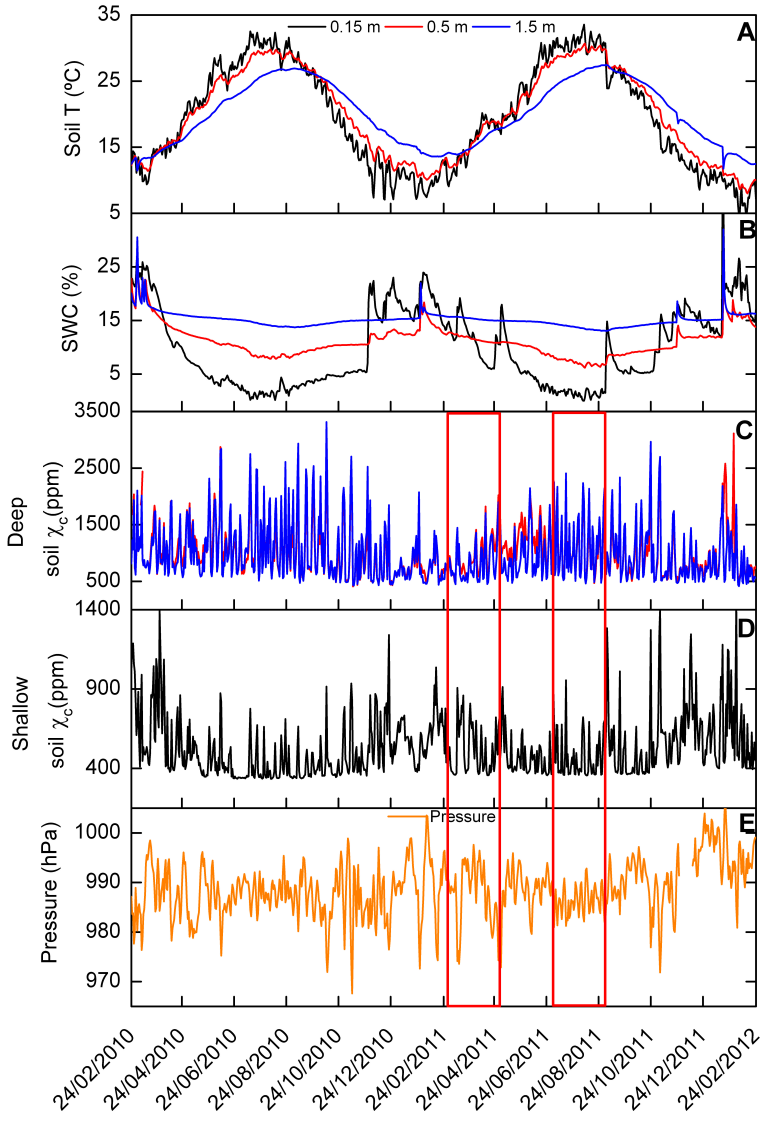

Fig. 1. Average daily values at soil depths of 0.15 m (black), 0.5 m (red) and 1.5 m (blue) for **(A)** temperature, **(B)** volumetric soil water content, **(C)** deep-soil CO_2 molar fraction (χ_c) and **(D)** shallow-soil CO_2 molar fraction (χ_c), as well as **(E)** the atmospheric pressure (orange) over two years. The red rectangle delimits the period amplified in Fig. 2.

at 0.15 m). The soil temperature decreases with depth, showing values of 30.8 °C, 29.4 °C and 26.1 °C at 0.15 m, 0.5 m and 1.5 m, respectively, and for the same depths the soil water content increased from 1.4 % to 7.2 % and 13.7 %, respectively.

Comparing the growing period versus dry period, it is observed that the shallow sensor detects more χ_c during the growing period, whereas deep χ_c is higher during the dry period (Table 1). As is commonly found in semiarid sites, soil temperatures are higher in the dry period than in the growing period, as opposed to what occurs with the soil water content. The mean pressure (p) and friction velocity (u_*) are similar for both periods, while air temperature is 10 °C higher during the dry period.

The soil CO_2 molar fraction (χ_c) shows strong inverse correlation with atmospheric pressure (p) on synoptic scales throughout the whole study period, as exemplified for four selected months (Fig. 2). Increments in χ_c correspond to decreases in p and vice versa both in the growing period (Fig. 2a) and in the dry period (Fig. 2b). The changes in the magnitude of p are higher in the growing period than in the dry period; however the variability in χ_c is lower in the growing period. Approximately every 3 days important changes occur in deep χ_c, with nearly identical values and trends at 0.5 and 1.5 m. Shallow χ_c has a similar trend, in that the highest peaks occur on the same days; however not all deep χ_c peaks correspond to maxima near the surface (e.g. 22 July and 31 July). Such inverse correlation between χ_c

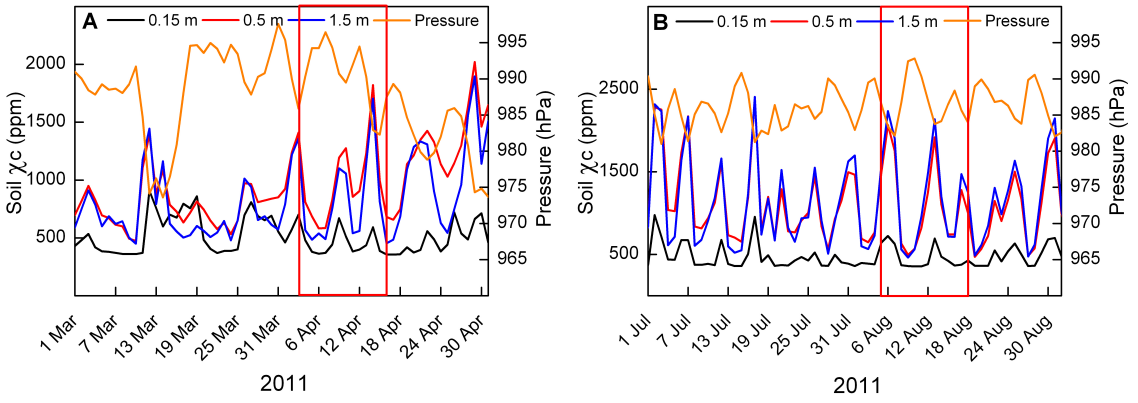

Fig. 2. Average daily values at 0.15 m (black), 0.5 m (red) and 1.5 m (blue) depth of soil CO_2 molar fraction (χ_c) and atmospheric pressure (orange) during two months for the growing period (panel A, March–April) and dry period (panel B, July–August). The red rectangle delimits the period amplified in Fig. 3.

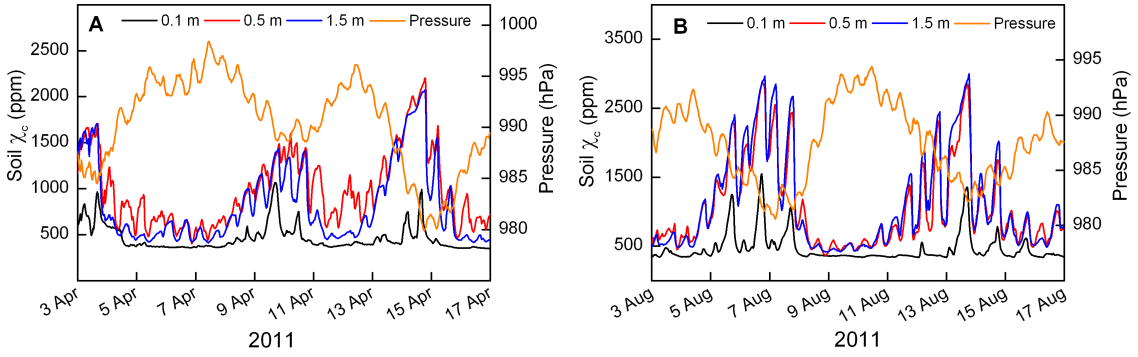

Fig. 3. Average half-hour values at 0.15 m, 0.5 m and 1.5 m depth of soil CO_2 molar fraction (χ_c) and atmospheric pressure for a period of 14 days during the growing period (panel A, April) and dry period (panel B, August).

and p extends to shorter timescales during the two vegetative periods, which will now be seen in higher resolution data corresponding to the red rectangles in Fig. 2.

3.3 Daily patterns

The deep-soil CO_2 molar fraction (χ_c) can jump to more than triple its mean value within a few hours, and shows inverse correlation with pressure (p) even at hourly timescales. Half-hour resolution data show that both p and deep χ_c (0.5 and 1.5 m) display two cycles per day, both during the growing season (Fig. 3a) and in the dry season (Fig. 3b). Excepting synoptic pressure changes such as the events on 14 April and 8 August, pressure typically has semi-diurnal changes with an amplitude of ca. 3 hPa. Deep χ_c shows a similar pattern with clear periodicity and two cycles per day, but some days have an amplitude up to 2000 ppm in a few hours (14 August) during this period of modest deep χ_c variability (cf. Figs. 1 and 2). However, shallow χ_c shows no such clear cyclic behavior.

Environmental factors that correlate with χ_c are summarized in Table 2 for the growing and dry periods, respectively. During the growing period, the shallow χ_c (0.15 m) shows correlation with T at 1.5 m and SWC at 0.5 m (R^2 of 0.25 and 0.37, respectively). Whereas for deep χ_c (0.5 m and 1.5 m) the main factor implicated are P and SWC at 0.5 m (R^2 of 0.39 and 0.50, respectively). During the dry period, shallow χ_c variations show maximum correlation with u_*, T and SWC at 0.15 m (R^2 of 0.29, 0.28 and 0.23, respectively). For deep χ_c the maximum correlations are found only with p (R^2 of 0.46).

Subterranean χ_c variations and correlation with atmospheric tides (0.5 days), synoptic events (3 days) and u_* are shown in the Table 3. During the growing period, u_* does not show correlation with χ_c variations at any depth, however deep χ_c variations show correlation with p on synoptic timescales increasing with depth (R^2 of 0.35 and 0.43 at 0.5 m and 1.5 m, respectively) and on daily timescales only at 1.5 m (R^2 of 0.23). During the dry period, shallow χ_c variations show high correlation with u_* whereas deep χ_c variations show high correlations with pressure both on synoptic

Table 2. Correlation coefficients (R^2) during both the growing period and the dry period between soil CO_2 molar fractions (χ_c) at three depths (0.15, 0.5 and 1.5 m), versus environmental parameters: friction velocity (u_*), pressure (p) and soil temperatures (T) and soil water contents (SWC) at the same three depths. Highlighted values denote the highest magnitudes for each depth.

	Growing period			Dry period		
	0.15 m	0.5 m	1.5 m	0.15 m	0.5 m	1.5 m
u_*	0.08	0.17	0.01	0.23	0.06	0.06
p	0	0.13	**0.39**	0.18	**0.46**	**0.43**
T 0.1	0.01	0.13	0	**0.29**	0.11	0.12
SWC 0.1 m	0.08	0.26	0.05	0.28	0.11	0.12
T 0.5	0.17	0.27	0.2	0.02	0.02	0
SWC 0.5 m	**0.37**	**0.50**	0.27	0.01	0.02	0
T 1.5	0.25	0.28	0.1	0.01	0.03	0
SWC 1.5 m	0.02	0.02	0	0.01	0.04	0

timescale (R^2 of 0.49 and 0.50 at 0.5 m and 1.5 m, respectively) and on daily timescales (R^2 of 0.4 and 0.45 at 0.5 m and 1.5 m, respectively).

3.4 Coupling deep-soil CO_2 variations with the atmosphere

Ecosystem-scale CO_2 exchanges (F_C) are shown during the growing period (6–17 April 2011) together with the soil CO_2 molar fraction (χ_c) at different depths in Fig. 4. Positive fluxes indicate emissions to the atmosphere and negative fluxes indicate uptake, so that during this period the ecosystem acts as a carbon sink. Over the week presented, the daily minima in F_C (corresponding to maximum uptake), coincide with the variations in χ_c. Days with high soil χ_c (9, 10, 13 and 14 of April) correspond to lower CO_2 uptake during daytime (Fig. 4).

The week presented was sunny with typical variation in the air temperature and no rain (data not shown), so the Fc variations cannot be attributed to changing physiological drivers. Figure 5 shows the ecosystem light response using the hyperbolic model described in the Eq. (2), distinguishing between days with decreasing versus increasing atmospheric pressures (Figs. 3a and 4). Table 4 shows parameters obtained from ecosystem light response curves; for both days with decreasing and increasing p, the canopy light utilization efficiency (α) and the ecosystem respiration (γ) are similar, however the maximum CO_2 uptake rate of the canopy at light saturation (β) increased by 43 % during days with increasing pressure.

4 Discussion

Variations in these deep-soil CO_2 molar fractions (χ_c) are due, not to biology, but rather to physical factors, most notably changes in pressure (p). These variations can be divided into two scales: the seasonal scale (Fig. 1), where deep

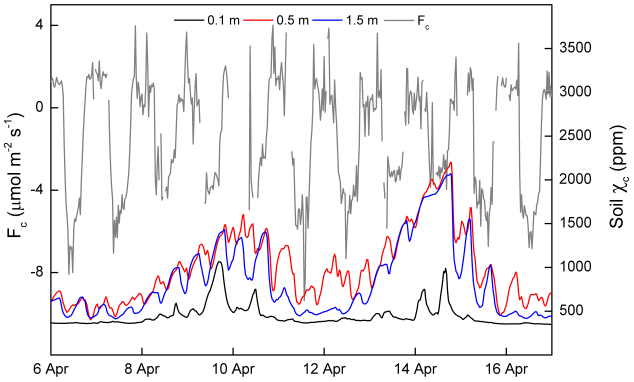

Fig. 4. Average half-hour values at 0.15 m (black), 0.5 m (red) and 1.5 m (blue) depth of soil CO_2 molar fraction (χ_c) and ecosystem-scale CO_2 fluxes (gray) measured by eddy covariance (F_C; negative values represent uptake).

Table 3. Correlation coefficients (R^2) with normalized variables during both the growing period and the dry period (Fig. 2) between soil CO_2 molar fractions (χ_c) at three depths (0.15, 0.5 and 1.5 m), on timescales of 0.5 days and 3 days, versus pressure (p) and the friction velocity (u_*).

		Growing period		Dry period	
Depth	Window (Days)	u_*	p	u_*	p
0.15 m	0.5	0	0	0.53	0
	3	0.01	0.13	0.24	0.14
0.5 m	0.5	0.01	0.06	0.04	0.4
	3	0	0.35	0.05	0.49
1.5 m	0.5	0.05	0.23	0.08	0.45
	3	0	0.43	0.06	0.5

χ_c correlates with soil temperature (T) and is inversely correlated to soil water content (SWC); and shorter – synoptic and hourly – scales (Figs. 2 and 3), where deep χ_c is clearly inversely correlated with p and can increment by a factor of four in a few hours. This behavior of deep χ_c is in contrast with that of shallow χ_c, which on seasonal scales (Fig. 1) is better described in terms of commonly reported semi-arid conditions where soil respiration is clearly restricted by drought (Barron-Gafford et al., 2011; Maranon-Jimenez et al., 2011; Oyonarte et al., 2012; Rey et al., 2011), showing an inverse correlation with T and correlation with SWC. Shallow χ_c shows maxima in winter and minima in summer coinciding with the vegetation's active period (Rey et al., 2012a) and favored by higher soil water contents limiting soil gas diffusivity. The similar behavior of the two deep sensors suggests that the deep pore spaces are highly interconnected, at least within the same caliche horizon.

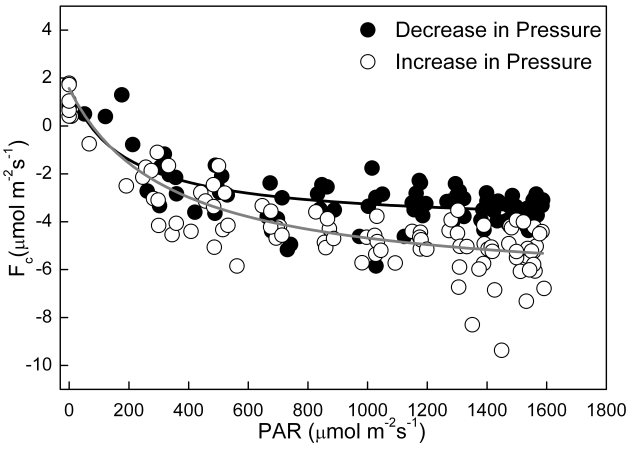

Fig. 5. Ecosystem light response curves. Daytime ecosystem CO_2 flux (F_C, μmol m^{-2} s^{-1}) versus the flux of photosynthetically active radiation (PAR; μmol m^{-2} s^{-1}) for days from Figs. 3a and 4 falling into two categories: days with decreasing atmospheric pressure and increasing deep-soil CO_2 (black circles; 9, 10, 13, 14 April) and vice versa (white circles; 11, 12, 15, 16 April). No changes in daily patterns of physiological drivers (temperature, relative humidity, net radiation or soil water content) were observed over the selected days.

Table 4. Parameters obtained from ecosystem light response curves shown in Fig. 5. Where α (μmol CO_2 J^{-1}) is the canopy light utilization efficiency and represents the initial slope of the light-response curve, β (μmol CO_2 m^{-2} s^{-1}) is the maximum CO_2 uptake rate of the canopy at light saturation and γ (μmol CO_2 m^{-2} s^{-1}) is the ecosystem respiration during the day.

Days	α	β	γ
Decreasing pressure	–0.032 ± 0.007	–5.8 ± 0.3	1.6 ± 0.2
Increasing pressure	–0.025 ± 0.006	–8.3 ± 0.5	1.6 ± 0.3

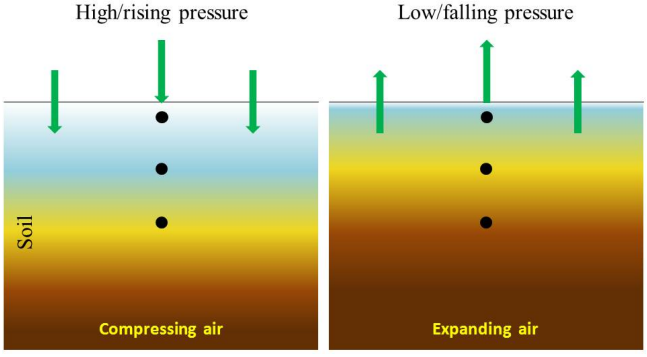

Fig. 6. Schematic of CO transport in soil air layers **(a)** compressing under high / rising synoptic pressure, and **(b)** expanding under low/falling pressure. High CO_2 molar fractions 2 are denoted in brown and low values in blue.

Such large variations in deep χ_c have no direct biological explanation, but suggest an underlying CO_2 reservoir in communication with the surface, depending on factors such as p, u_* or SWC. The origin of the CO_2 reservoir could be either geothermal (i.e., magmatic or metamorphic; Rey et al., 2012b) or biological in origin. Geothermal sources may exist at a depth below Balsa Blanca because the site is located over a large active tectonic fault system. Biological origins would be due to CO_2 storage in deep layers resulting from plant activity and microbes, whose metabolic activities might well be affected by the large variations in χ_c (a secondary effect, at most). The CO_2 respired in the root zone increases air density (Sanchez-Canete et al., 2013; Kowalski and Sanchez-Canete, 2010), and so enables gravitational percolation through the pore space toward deeper layers where it can be stored.

Although in this study, p is the main factor implicated in deep χ_c variations, Fig. 1 shows that χ_c variability is greater in summer when p variations are reduced. This highlights the important role of SWC in CO_2 exchange: despite greater synoptic pressure variability, winter has lower χ_c variations because soil pores are filled with water, limiting gas flows. In summer, by contrast, ventilation is facilitated by dry soil conditions with gas-filled pore space (Cuezva et al., 2011; Maier et al., 2010). This would allow superficial CO_2 values to increase during the dry season because soil pore space opens to the flow of CO_2-rich air from the deep soil to near-surface layers.

At synoptic scales, passing frontal systems cause increases / decreases in p leading to fourfold decreases / increases in deep χ_c (Fig. 2). Such variability can only be explained by CO_2 transported from depth towards the surface. A simple model to explain the role of pressure (p) in subterranean CO_2 transport is shown in Fig. 6. When p increases, the soil air is compressed and atmospheric air penetrates into the soil decreasing the deep χ_c. Similarly, when p decreases, the soil air expands increasing the deep χ_c since deeper soil air distends toward the surface.

Hourly timescales (Fig. 3) show clear inverse correlation between the deep χ_c and p, where even small daily p oscillations (3 hPa) due to twice daily atmospheric tides (Lindzen, 1979) generate large variations in χ_c at depth (2000 ppm; e.g., falling χ_c on 12 August, Fig. 3b). Deep-soil χ_c (0.5 and 1.5 m) shows two cycles per day, in rhythm with p, whereas shallow χ_c has just one. Shallow χ_c is more affected by friction velocity (Table 3) because it is in the upper part of the soil, and thus more easily ventilated decreasing χ_c (Hirsch et al., 2004; Sanchez-Canete et al., 2011). Similarly, Rey et al. (2012a) concluded that the wind was the main driver of the net ecosystem carbon balance at this experimental site. At a nearby ecosystem with carbonate soils, such subterranean ventilation represented up to 62 % of the annual emissions during dry periods (Perez-Priego et al., 2013).

The effects of emissions from deep CO_2 soil were registered in the atmosphere, driven by synoptic pressure changes. The light response curves demonstrated that on both consecutive and non-consecutive days and near-constant environmental conditions (temperature, relative humidity, net radiation and soil water content), the maximum downward CO_2 flux toward the canopy at light saturation increased by 43 % during days with increasing synoptic pressure, versus those with falling pressure. This is in accordance with the explanatory diagram of Fig. 6. With rising pressure, part of the CO_2 respired by plants tends to accumulate in the soil, registering more negative eddy fluxes and therefore obtaining a high value of β, which might be interpreted erroneously as the maximum CO_2 uptake rate of the canopy at light saturation (as in Eq. 2). However, with falling pressure, both CO_2 stored in the soil and that respired by plants is emitted to the atmosphere, making eddy fluxes less negative and lowering the value of β. The results presented in this paper come from a vertical CO_2 profile of three depths without horizontal replication but with a long and continuous data series. For this reason, the results invite further research at this and other semiarid ecosystems regarding the influence of synoptic pressure changes on variations in deep-soil CO_2 molar fractions at different locations, and their role on the net ecosystem carbon balance.

5 Conclusions

This study reveals that during both growing periods and dry periods, variations in the deep-soil CO_2 molar fraction (χ_c) are due predominantly to atmospheric pressure (p) variations and not directly to biological influences. In a few hours, the deep χ_c can increase or decrease fourfold, highlighting the need for continuous (versus sporadic) monitoring of soil CO_2 effluxes. Deep χ_c has a pattern with two cycles per day, due to p oscillations caused by atmospheric tides. Nonetheless shallow χ_c has a pattern with one cycle per day, due to its dependence mainly on the friction velocity during the dry period and on biological factors during both dry and growing periods, showing maxima for this semiarid ecosystem when soil water content is not limiting, with temperature dependence as well. The effects of emissions from deep-soil CO_2 were registered in the atmosphere driven by synoptic pressure changes: on days with rising pressure the downward CO_2 flux is higher than days with falling pressure because on these days CO_2 respired by plants accumulates in the soil. Future studies focused on determining the net ecosystem carbon balance should not rely exclusively on Fick's law to calculate soil CO_2 effluxes from profile data.

Acknowledgements. This research was funded by the Andalusian regional government project GEOCARBO (P08-RNM-3721) and GLOCHARID, including European Union ERDF funds, with support from Spanish Ministry of Science and Innovation projects Carbored-II (CGL2010-22193-C04-02), SOILPROF (CGL2011-15276-E) and CARBORAD (CGL2011-27493), as well as the European Community's Seventh Framework Programme (FP7/2007-2013) under grant agreement no. 244122. We wish to thank Cecilio Oyonarte for useful comments on the manuscript. We thank three anonymous reviewers for their constructive comments.

Edited by: G. Wohlfahrt

References

Barron-Gafford, G. A., Scott, R. L., Jenerette, G. D., and Huxman, T. E.: The relative controls of temperature, soil moisture, and plant functional group on soil CO_2 efflux at diel, seasonal, and annual scales, J. Geophys. Res.-Biogeosci., 116, G01023, doi:10.1029/2010jg001442, 2011.

Bowling, D. R. and Massman, W. J.: Persistent wind-induced enhancement of diffusive CO_2 transport in a mountain forest snowpack, J. Geophys. Res.-Biogeosci., 116, G04006, doi:10.1029/2011jg001722, 2011.

Chapin, F. S., Woodwell, G. M., Randerson, J. T., Rastetter, E. B., Lovett, G. M., Baldocchi, D. D., Clark, D. A., Harmon, M. E., Schimel, D. S., Valentini, R., Wirth, C., Aber, J. D., Cole, J. J., Goulden, M. L., Harden, J. W., Heimann, M., Howarth, R. W., Matson, P. A., McGuire, A. D., Melillo, J. M., Mooney, H. A., Neff, J. C., Houghton, R. A., Pace, M. L., Ryan, M. G., Running, S. W., Sala, O. E., Schlesinger, W. H., and Schulze, E. D.: Reconciling carbon-cycle concepts, terminology, and methods, Ecosystems, 9, 1041–1050, doi:10.1007/s10021-005-0105-7, 2006.

Clements, W. and Wilkening, M.: Atmospheric pressure effects on ^{222}Rn transport across the earth-air interface, J. Geophys. Res., 79, 5025–5029, 1974.

Comas, X., Slater, L., and Reeve, A.: Spatial variability in biogenic gas accumulations in peat soils is revealed by ground penetrating radar (GPR), Geophys. Res. Lett., 32, L08401, doi:10.1029/2004gl022297, 2005.

Comas, X., Slater, L., and Reeve, A.: In situ monitoring of free-phase gas accumulation and release in peatlands using ground penetrating radar (GPR), Geophys. Res. Lett., 34, L06402, doi:10.1029/2006gl029014, 2007.

Comas, X., Slater, L., and Reeve, A. S.: Atmospheric pressure drives changes in the vertical distribution of biogenic free-phase gas in a northern peatland, J. Geophys. Res.-Biogeo., 116, G04014, doi:10.1029/2011jg001701, 2011.

Cuezva, S., Fernandez-Cortes, A., Benavente, D., Serrano-Ortiz, P., Kowalski, A. S., and Sanchez-Moral, S.: Short-term CO_2(g) exchange between a shallow karstic cavity and the external atmosphere during summer: Role of the surface soil layer, Atmos. Environ., 45, 1418–1427, doi:10.1016/j.atmosenv.2010.12.023, 2011.

Emmerich, E. W.: Carbon dioxide fluxes in a semiarid environment with high carbonate soils, Agric. For. Meteorol., 116, 91–102, 2003.

Falge, E., Baldocchi, D., Olson, R., Anthoni, P., Aubinet, M., Bernhofer, C., Burba, G., Ceulemans, R., Clement, R., Dolman, H., Granier, A., Gross, P., Grunwald, T., Hollinger, D., Jensen, N. O., Katul, G., Keronen, P., Kowalski, A., Lai, C. T., Law, B. E., Meyers, T., Moncrieff, H., Moors, E., Munger, J. W., Pilegaard, K., Rannik, U., Rebmann, C., Suyker, A., Tenhunen, J., Tu, K., Verma, S., Vesala, T., Wilson, K., and Wofsy, S.: Gap filling strategies for defensible annual sums of net ecosystem exchange, Agric. For. Meteorol., 107, 43–69, doi:10.1016/s0168-1923(00)00225-2, 2001.

Falge, E., Baldocchi, D., Tenhunen, J., Aubinet, M., Bakwin, P., Berbigier, P., Bernhofer, C., Burba, G., Clement, R., Davis, K. J., Elbers, J. A., Goldstein, A. H., Grelle, A., Granier, A., Guomundsson, J., Hollinger, D., Kowalski, A. S., Katul, G., Law, B. E., Malhi, Y., Meyers, T., Monson, R. K., Munger, J. W., Oechel, W., Paw, K. T., Pilegaard, K., Rannik, U., Rebmann, C., Suyker, A., Valentini, R., Wilson, K., and Wofsy, S.: Seasonality of ecosystem respiration and gross primary production as derived from FLUXNET measurements, Agric. For. Meteorol., 113, 53–74, 2002.

Fujiyoshi, R., Haraki, Y., Sumiyoshi, T., Amano, H., Kobal, I., and Vaupotic, J.: Tracing the sources of gaseous components (Rn^{-222}, CO_2 and its carbon isotopes) in soil air under a cool-deciduous stand in Sapporo, Japan, Environ. Geochem. Health, 32, 73–82, doi:10.1007/s10653-009-9266-1, 2010.

Granieri, D., Chiodini, G., Marzocchi, W., and Avino, R.: Continuous monitoring of CO_2 soil diffuse degassing at Phlegraean Fields (Italy): influence of environmental and volcanic parameters, Earth Planet. Sci. Lett., 212, 167–179, doi:10.1016/s0012-821x(03)00232-2, 2003.

Hirsch, A. I., Trumbore, S. E., and Goulden, M. L.: The surface CO_2 gradient and pore-space storage flux in a high-porosity litter layer, Tellus B, 56, 312–321, doi:10.1111/j.1600-0889.2004.00113.x, 2004.

Huwald, H., Selker, J. S., Tyler, S. W., Calaf, M., van de Giesen, N. C., and Parlange, M. B.: Carbon monoxide as a tracer of gas transport in snow and other natural porous media, Geophys. Res. Lett., 39, L02504, doi:10.1029/2011gl050247, 2012.

Kowalski, A. S., Anthoni, P. M., Vong, R. J., Delany, A. C., and Maclean, G. D.: Deployment and evaluation of a system for ground-based measurement of cloud liquid water turbulent fluxes, Journal of Atmospheric and Oceanic Technology, 14, 468–479, doi:10.1175/1520-0426(1997)014<0468:daeoas>2.0.co;2, 1997.

Kowalski, A. S., Serrano-Ortiz, P., Janssens, I. A., Sanchez-Moraic, S., Cuezva, S., Domingo, F., Were, A., and Alados-Arboledas, L.: Can flux tower research neglect geochemical CO_2 exchange?, Agric. For. Meteorol., 148, 1045-1054, doi:10.1016/j.agrformet.2008.02.004, 2008.

Kowalski, A. S. and Sanchez-Canete, E. P.: A New Definition of the Virtual Temperature, Valid for the Atmosphere and the CO_2-Rich Air of the Vadose Zone, J. Appl. Meteorol. Climatol., 49, 1692–1695, doi:10.1175/2010jamc2534.1, 2010.

Lewicki, J. L., Hilley, G. E., Tosha, T., Aoyagi, R., Yamamoto, K., and Benson, S. M.: Dynamic coupling of volcanic CO_2 flow and wind at the Horseshoe Lake tree kill, Mammoth Mountain, California, Geophys. Res. Lett., 34, L03401, doi:10.1029/2006gl028848, 2007.

Lewicki, J. L., Fischer, M. L., and Hilley, G. E.: Six-week time series of eddy covariance CO_2 flux at Mammoth Mountain, California: Performance evaluation and role of meteorological forcing, J. Volcanol. Geotherm. Res., 171, 178–190, doi:10.1016/j.jvolgeores.2007.11.029, 2008.

Lindzen, R. S.: Atmospheric tides, Annu. Rev. Earth Planet. Sci., 7, 199–225, doi:10.1146/annurev.ea.07.050179.001215, 1979.

Maier, M., Schack-Kirchner, H., Hildebrand, E. E., and Holst, J.: Pore-space CO_2 dynamics in a deep, well-aerated soil, European Journal of Soil Science, 61, 877–887, doi:10.1111/j.1365-2389.2010.01287.x, 2010.

Maranon-Jimenez, S., Castro, J., Kowalski, A. S., Serrano-Ortiz, P., Reverter, B. R., Sanchez-Canete, E. P., and Zamora, R.: Post-fire soil respiration in relation to burnt wood management in a Mediterranean mountain ecosystem, Forest Ecol. Manage., 261, 1436–1447, doi:10.1016/j.foreco.2011.01.030, 2011.

Maier, M., Schack-Kirchner, H., Aubinet, M., Goffi, S., Longdoz, B., and Parent, F.: Turbulence Effect on Gas Transport in Three Contrasting Forest Soils, Soil Sci. Soc. Am. J., 76, 1518–1528, doi:10.2136/sssaj2011.0376, 2012.

Massman, W. J., Sommerfeld, R. A., Mosier, A. R., Zeller, K. F., Hehn, T. J., and Rochelle, S. G.: A model investigation of turbulence-driven pressure-pumping effects on the rate of diffusion of CO_2, N_2O, and CH_4 through layered snowpacks, J. Geophys. Res.-Atmos., 102, 18851–18863, doi:10.1029/97jd00844, 1997.

Mielnick, P., Dugas, W. A., Mitchell, K., and Havstad, K.: Long-term measurements of CO_2 flux and evapotranspiration in a Chihuahuan desert grassland, J. Arid. Environ., 60, 423–436, doi:10.1016/j.jaridenv.2004.06.001, 2005.

Nachshon, U., Dragila, M., and Weisbrod, N.: From atmospheric winds to fracture ventilation: Cause and effect, J. Geophys. Res.-Biogeosci., 117, G02016, doi:10.1029/2011jg001898, 2012.

Oyonarte, C., Rey, A., Raimundo, J., Miralles, I., and Escribano, P.: The use of soil respiration as an ecological indicator in arid ecosystems of the SE of Spain: Spatial variability and controlling factors, Ecol. Indic., 14, 40–49, doi:10.1016/j.ecolind.2011.08.013, 2012.

Perez-Priego, O., Serrano-Ortiz, P., Sanchez-Canete, E. P., Domingo, F., and Kowalski, A. S.: Isolating the effect of subterranean ventilation on CO_2 emissions from drylands to the atmosphere, Agric. For. Meteorol., 180, 194–202, doi:10.1016/j.agrformet.2013.06.014, 2013.

Plestenjak, G., Eler, K., Vodnik, D., Ferlan, M., Cater, M., Kanduc, T., Simoncic, P., and Ogrinc, N.: Sources of soil CO_2 in calcareous grassland with woody plant encroachment, J. Soils Sedim., 12, 1327–1338, doi:10.1007/s11368-012-0564-3, 2012.

Reicosky, D. C., Gesch, R. W., Wagner, S. W., Gilbert, R. A., Wente, C. D., and Morris, D. R.: Tillage and wind effects on soil CO_2 concentrations in muck soils, Soil Tillage Res., 99, 221–231, doi:10.1016/j.still.2008.02.006, 2008.

Rey, A., Pegoraro, E., Oyonarte, C., Were, A., Escribano, P., and Raimundo, J.: Impact of land degradation on soil respiration in a steppe (Stipa tenacissima L.) semi-arid ecosystem in the SE of Spain, Soil Biol. Biochem., 43, 393–403, doi:10.1016/j.soilbio.2010.11.007, 2011.

Rey, A., Belelli-Marchesini, L., Were, A., Serrano-Ortiz, P., Etiope, G., Papale, D., Domingo, F., and Pegoraro, E.: Wind as a main driver of the net ecosystem carbon balance of a semiarid Mediter-

ranean steppe in the South East of Spain, Glob. Change Biol., 18, 539–554, doi:10.1111/j.1365-2486.2011.02534.x, 2012a.

Rey, A., Etiope, G., Belelli-Marchesini, L., Papale, D., and Valentini, R.: Geologic carbon sources may confound ecosystem carbon balance estimates: Evidence from a semiarid steppe in the southeast of Spain, J. Geophys. Res.-Biogeo., 117, G03034, doi:10.1029/2012JG001991, 2012b.

Rogie, J. D., Kerrick, D. M., Sorey, M. L., Chiodini, G., and Galloway, D. L.: Dynamics of carbon dioxide emission at Mammoth Mountain, California, Earth Planet. Sci. Lett., 188, 535–541, doi:10.1016/s0012-821x(01)00344-2, 2001.

Sanchez-Canete, E. P., Serrano-Ortiz, P., Kowalski, A. S., Oyonarte, C., and Domingo, F.: Subterranean CO_2 ventilation and its role in the net ecosystem carbon balance of a karstic shrubland, Geophys. Res. Lett., 38, L09802, doi:10.1029/2011gl047077, 2011.

Sanchez-Canete, E. P., Serrano-Ortiz, P., Domingo, F., and Kowalski, A. S.: Cave ventilation is influenced by variations in the CO_2-dependent virtual temperature, Int. J. Speleol., 42, 1–8, doi:10.5038/1827-806X.42.1.1, 2013.

Seok, B., Helmig, D., Williams, M. W., Liptzin, D., Chowanski, K., and Hueber, J.: An automated system for continuous measurements of trace gas fluxes through snow: an evaluation of the gas diffusion method at a subalpine forest site, Niwot Ridge, Colorado, Biogeochemistry, 95, 95–113, doi:10.1007/s10533-009-9302-3, 2009.

Serrano-Ortiz, P., Domingo, F., Cazorla, A., Were, A., Cuezva, S., Villagarcia, L., Alados-Arboledas, L., and Kowalski, A. S.: Interannual CO_2 exchange of a sparse Mediterranean shrubland on a carbonaceous substrate, J. Geophys. Res.-Biogeo., 114, G04015, doi:10.1029/2009jg000983, 2009.

Serrano-Ortiz, P., Roland, M., Sanchez-Moral, S., Janssens, I. A., Domingo, F., Godderis, Y., and Kowalski, A. S.: Hidden, abiotic CO_2 flows and gaseous reservoirs in the terrestrial carbon cycle: Review and perspectives, Agric. For. Meteorol., 150, 321–329, doi:10.1016/j.agrformet.2010.01.002, 2010.

Stull, R. B.: An Introduction to Boundary Layer Meteorology, Kluwer Academic Publishers, Dordrecht, 1988.

Subke, J. A., Reichstein, M., and Tenhunen, J. D.: Explaining temporal variation in soil CO_2 efflux in a mature spruce forest in Southern Germany, Soil Biol. Biochem., 35, 1467–1483, doi:10.1016/s0038-0717(03)00241-4, 2003.

Takle, E. S., Massman, W. J., Brandle, J. R., Schmidt, R. A., Zhou, X. H., Litvina, I. V., Garcia, R., Doyle, G., and Rice, C. W.: Influence of high-frequency ambient pressure pumping on carbon dioxide efflux from soil, Agric. For. Meteorol., 124, 193–206, doi:10.1016/j.agrformet.2004.01.014, 2004.

Webb, E. K., Pearman, G. I., and Leuning, R.: Correction of flux measurements for density effects due to heat and water vapor transfer, Q. J. R. Meteorol. Soc., 106, 85–100, 1980.

Weisbrod, N., Dragila, M., Nachson, U., and Pillersdorf, M.: Falling through the cracks: the role of fractures in Earth-atmosphere gas exchange, Geophys. Res. Lett., 36, L02401, doi:10.1029/2008GL036096, 2009.

Were, A., Serrano-Ortiz, P., de Jong, C. M., Villagarcia, L., Domingo, F., and Kowalski, A. S.: Ventilation of subterranean CO_2 and Eddy covariance incongruities over carbonate ecosystems, Biogeosciences, 7, 859–867, doi:10.5194/bg-7-859-2010, 2010.

Wilks, D. S.: Statistical Methods in the Atmospheric Sciences, 2 Edn., Academic Press, 649 pp., 2006.

WRB: World Reference Base for Soil Resources 2006, World Soil Resources Reports No. 103. FAO, Rome, 128 pp., 2006.